ORIGINAL RESEARCH ARTICLE

Relationship between stimulus size and different components of the electroretinogram (ERG) elicited by flashed stimuli

Mathias G. Nittmann · Avinash J. Aher · Jan Kremers ⓘ · Radouil Tzekov ⓘ

Abstract

Purpose To investigate how light stimulus conditions of varying spatial sizes affect components of the flash and long-flash electroretinogram (ERG) in normal subjects.

Method Three stimulus conditions were generated by a Ganzfeld stimulator: a white flash on white background (WoW), a red flash on a blue background (RoB) and an L+M-cone isolating on–off (long flash) stimulus (Cone Iso). ERGs were recorded from six subjects (5 M, 1 F) with DTL electrodes to full-field (FF), 70°, 60°, 50°, 40°, 30° and 20° diameter circular stimuli. Amplitudes and peak times for a-, b-, d- and i-wave, and PhNR were examined. PhNR amplitudes were estimated in two different ways: from baseline (fB) and from preceding b-wave peak (fP).

Results With decreasing stimulus size, amplitudes for all ERG waveform components attenuated and peak times increased, although the effect varied across different components. An exponential fit described the relationship between amplitudes and size of stimulated retinal area well for most components and conditions ($R^2 = 0.75$-0.99), except for PhNR(fB) ($R^2 = -0.16$–0.88). For peak times, an exponential

M. G. Nittmann · R. Tzekov
Department of Ophthalmology, University of South Florida, 13330 USF Laurel Dr, Tampa,
FL 33612, USA

A. J. Aher · J. Kremers
Department of Ophthalmology, University Hospital Erlangen, Schwabachanlage 6, 91054 Erlangen, Germany

J. Kremers
Department of Anatomy II, University of Erlangen-Nürnberg, Universitätsstr. 19, 91054 Erlangen, Germany

J. Kremers
School of Optometry and Vision Science, University of Bradford, Richmond Rd,
Bradford, West Yorkshire BD7 1DP, UK

R. Tzekov
Department of Medical Engineering, University of South Florida, 4202 E. Fowler Avenue, ENG 030, Tampa,
FL 33620, USA

R. Tzekov
James A Haley Veterans' Hospital, 13000 Bruce B. Downs Blvd., Tampa, FL 33612, USA

R. Tzekov
The Roskamp Institute, 2040 Whitfield Ave, Sarasota,
FL 34243, USA

R. Tzekov (✉)
USF Eye Institute, 12901 Bruce B. Downs Blvd., MDC 21, Tampa, FL 33612, USA
e-mail: rtzekov@usf.edu

decay function also fitted the data well (R^2= 0.81–0.97), except in a few cases where the exponential constant was too small and a linear regression function was applied instead (a-wave Cone Iso, b- and i-wave WoW). The exponential constants for RoB amplitudes (b-wave, PhNR(fB), PhNR(fP)) were larger compared to their counterparts under WoW ($p < 0.05$), while there was no difference between the constants for a-wave amplitudes and peak times and for PhNR peak times. The exponential constants of amplitudes vs. area under WoW and Cone Iso were remarkably similar, while under RoB PhNR(fB) showed larger constants compared to either a- or b-wave ($p < 0.05$).

Conclusion ERG components change in a predictable way with stimulus size and spectral characteristics of the stimulus under these conditions. This predictability could allow a modified version of these sets of stimuli to be tested for clinical applicability.

Keywords Electroretinogram · Stimulus size · Flash stimuli · Square wave stimuli · Photopic negative response

Introduction

The electroretinogram (ERG) reflects the electrical activity of the retina in response to light stimuli. The most widely used version is the full-field flash (FF) ERG, also referred to as a Ganzfeld ERG, where flashes of light stimulate the whole retina and the recorded signal represents a mass response, reflecting bioelectrical activity from the whole retina. The FF ERG signal consists of several components which may appear and change in relative size depending on stimulus conditions. Under light-adapted conditions, a typical human FF ERG waveform elicited by a white flash of intermediate strength (1–3 cd.s/m^2; top trace in Fig. 1a) consists of two negative components: an a-wave and a photopic negative response (PhNR), and two positive components: a b-wave and an i-wave. These components originate from different cellular subpopulations and reflect distinct physiological processes. Under these conditions, the light-adapted a-wave is believed to receive strong input from OFF-bipolar cells and some, likely small, direct contribution from cone photoreceptors [1, 2]. The

photopic b-wave is generated by a summation of ON- and OFF-bipolar cell activity [3], although some minor input from retinal ganglion cells may also exist [4]. The origins of the i-wave are still subject to some debate, although studies suggest that cone OFF-bipolar cell or cone off-inner retinal activity is the primary source [5–7]. A particularly clinically relevant component is the photopic negative response (PhNR), a corneal negative wave that appears after the positive b-wave peak under light-adapted conditions. The PhNR has been shown to predominantly reflect the spiking activity of retinal ganglion cells (RGCs) [8], and pathologies of the retinal ganglion cell layer, such as in glaucoma, cause attenuated PhNRs [9, 10].

The spectral characteristics of the flash stimulus may influence the elicited ERG waveforms. A broadband white flash on a white background is the traditional stimulus used for recording clinically standardized FF ERG [11]. However, a narrowband red flash on a narrowband blue background stimulus has been reported to produce larger PhNR amplitudes [12] and was recommended as stimulus for an extended protocol for PhNR recording [13]. Other studies reported that if the stimuli are photopically matched, the spectral composition has little influence for cone-driven ERGs [14].

There is evidence that the PhNR in responses to cone isolating stimuli with sawtooth temporal profiles is particularly large when stimulating the central retina in comparison with the a- and the b-wave [15]. It is unclear, if spatial differences between a- and b-wave on the one hand, and the PhNR on the other hand, are also present in the more conventional flash ERGs. The present study investigates the effect of stimulus size on the components of the commonly used FF ERGs when elicited by white flashes on a white background compared to those evoked by red flashes on a blue background. These are conditions where the spectral composition of the stimuli is fairly well described. The stimulus strength on L- and M-cones may, however, vary substantially. We therefore additionally studied the influence of stimulus size in long-flash conditions where L- and M-cones are selectively stimulated with equal strength (in terms of cone contrast) and in phase (i.e., resulting in simultaneous excitation increases and decreases in the two).

Although flash ERG studies of the PhNR have traditionally utilized full-field stimulation, some works have also shown utility of focal macular ERGs
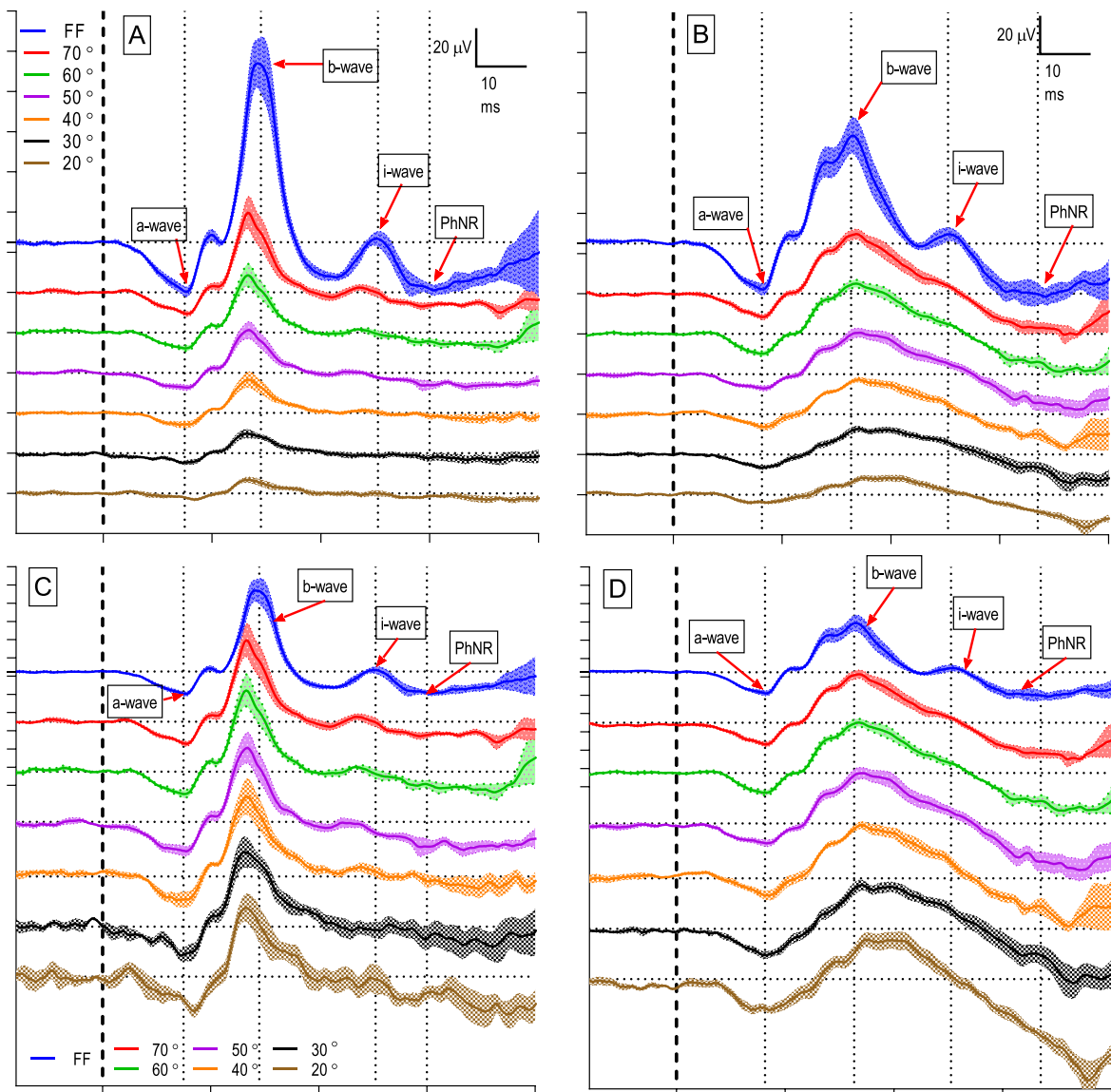
Fig. 1 Averaged ERG traces (± SEM) recorded from six subjects for the seven different stimulus configurations (FF and 70°, 60°, 50°, 40°, 30° and 20° diameter stimuli) are superimposed. **a** ERGs responses generated by white flash stimulus on a white background (WoW); **b** by red flash stimulus on a blue background (RoB); **c** ERG responses under WoW where the b-wave amplitude has been equalized for all stimulus sizes; **d** ERG responses under RoB with equalized b-wave amplitudes for all stimulus sizes. Dotted horizontal lines in each trace represent the baseline. The thick dotted vertical lines indicate the onset of flash stimulus. The thin dotted vertical lines indicate the time of each wave's peak occurrence for the FF stimulus (top row), allowing for comparison with smaller stimulus sizes (rows below). The nomenclature of the ERG components is also presented for FF, including the a-wave, b-wave, i-wave and PhNR

to independently evaluate each ERG component [16]. Indeed, later studies specifically demonstrated that detection sensitivity of the focal PhNR was significantly higher than that of the PhNR generated by a full-field stimulus in patients with early-stage glaucoma [17–19]. A study in monkeys using a red flash on blue background stimulus showed that the PhNR/b-wave amplitude ratio increased for focal ERG compared to full-field stimulation [20]. Hence, one way to improve our understanding of the PhNR and its

relationship to other ERG components (e.g., a-wave, b-wave) is to record ERGs to stimuli of different sizes. As the size of the stimulus decreases and approaches the size of the macula (~ 20 deg in diameter), it can be expected that the relative size of the PhNR in relationship to the b-wave will increase. This hypothesis is based on anatomical evidence that the ratio of RGCs to ON-bipolar cells (which are the major generator of the b-wave) increases from approximately 1:2 in the periphery of the macaque monkey retina, to nearly 1:1 in the central retina [21] and on the basis of the above-mentioned ERG data with cone isolating sawtooth stimuli.

Methods and subjects

Subjects

In the present study, ERGs were recorded from six healthy human observers aged between 22 and 58 years old (5 male, 1 female) at the Dept. of Ophthalmology of the University Hospital Erlangen, Germany. Three experimental procedures were employed, designated as white on white (WoW), red on blue (RoB) and cone isolating (Cone Iso), described in sub-section Visual Stimulation. The subjects did not have any history of eye disease and underwent a complete ophthalmological examination showing no ocular abnormalities. All participants had normal color vision as established with an anomaloscope (Oculus Optikgerate GmbH, Wetzlar, Germany). A written consent was obtained from all participants prior to the experiments, which followed the tenets of the Declaration of Helsinki. The protocols were approved by the institutional ethical committees of both the University Hospital Erlangen and the University of South Florida (Medical Faculty of the University of Erlangen-Nürnberg, Germany; Institutional Review Board of University of South Florida, USA).

ERG recordings

Full-field ERGs were recorded from the right eye of each subject using the RETIport Ganzfeld Q450 system (Roland Consult, Germany). The pupil was dilated with a drop of 0.5% tropicamide (Stulln Pharma GmbH, Germany). A custom-made DTL electrode [22] serving as active electrode was placed over the lower conjunctiva and attached near the inner and outer canthus. The skin of the ipsilateral temple and central forehead was cleaned with Nuprep skin preparing gel (D. O. Weaver & Co.), and two gold cup electrodes filled with electrode paste (Ten20 conductive, D. O. Weaver & Co., Aurora, Colorado, USA) were secured to these locations with medical-grade tape, serving as a reference and ground electrodes, respectively. The impedance of the electrodes was maintained below 5 kΩ. The subject's left eye was covered with a black opaque eye patch. Subjects rested their heads on a chin rest and were asked to fixate at a central red light emitting diode (LED) in the Ganzfeld stimulator (Q450SC, Roland Consult). Recorded ERGs were amplified by a factor of 10^6 and band pass filtered between 1 and 300 Hz. The brief flash ERG signals were sampled in 512 data points over 150-ms recording windows, resulting in a digitization rate of 3407 Hz. Sampling rate of the cone isolating conditions was 2048 Hz.

Visual stimulation

The visual stimuli were generated using the RETIport system (Roland Consult, Germany) and presented using an integrating Ganzfeld sphere (Q450SC, Roland Consult). The Ganzfeld sphere was equipped with six different LED arrays (primaries) each with a different emission spectrum. The mean luminance, waveform, contrast, relative phase and frequency of each LED array could be controlled independently with RETIport software.

Three different stimulus conditions were employed: white flashes on a white background (WoW), red flashes on a blue background (RoB) and L+M-cone isolating square wave (long flash) stimuli (Cone Iso). For WoW, the white flash was set to a strength of 2 cd.s/m^2 with CIE coordinates $x = 0.3361$, $y = 0.3486$, and the luminance of the white background was 25 cd/m^2, as recommended by the ISCEV standard for full-field light-adapted ERGs [11] . For RoB conditions, the red flash was set to a strength of 2 cd.s/m^2, with CIE coordinates $x = 0.1279$ and $y = 0.0759$, and the luminance of the blue background was 10 cd/m^2, as recommended by the ISCEV extended protocol for recordings of the PhNR [13]. The individual Michelson cone contrasts elicited by this red flash were as follows: S-cone: 1.4%, M-cone: 77.6%, L-cone 96.8%, rod: 8.4%.

Flash stimuli for white on white and red on blue conditions were administered every 5 s (stimulation rate: 0.2 Hz), and ERG responses were averaged over 16 epochs.

For the L- and M-cone isolating stimulus condition, the double silent substitution method was used. The silent substitution method allows for the control of L-cone, M-cone, S-cone and rod photoreceptor modulations independently [23, 24]. With known diode emission spectra and photoreceptor fundamentals, mean photoreceptor excitations (expressed in cone or rod Michelson contrasts) were calculated via a linear transformation [23, 25, 26]. In the present study, four primaries (red, green, blue and amber) were used for isolating L- and M-cone activities. The output peak wavelength $\pm$ half-bandwidth at half-height was 638 ± 9 nm for red, 523 ± 19 nm for green, 469 ± 11 nm for blue and 594 ± 8 nm for amber, respectively. The spectral characteristics, chromaticities and luminances of each class of LED were calibrated using a CAS 140 spectrophotometer (Instrument Systems, Germany). The L- and M-cones were modulated in phase (meaning that their excitation profiles were identical and not time shifted relative to each other) both with 42% cone contrast, while rod and S-cones were silenced. The individual luminances of the four primaries were 20, 10, 1 and 40 cd/m2 for red, green, blue and amber, respectively, which resulted in a reddish mean chromaticity with CIE coordinates: $x = 0.5674$, $y = 0.3772$. The mean luminance of L+M-cone isolating stimuli was 71 cd/m^2 (i.e., 3500 photopic Td retinal illuminance, assuming an 8 mm pupil diameter). The L- and M-cone isolating stimulus was administered as a 2 Hz square wave (corresponding to a 250 ms long flash), and ERG responses were averaged over 80 epochs each lasting one second. To avoid onset artifacts, the initial 2 s of recording after start of the stimulus was discarded.

For each stimulus condition, ERG responses were recorded for seven different spatial configurations: full-field (FF) and 70°, 60°, 50°, 40° 30° and 20° diameter stimuli [27, 28]. The spatial stimulus configurations were created using cardboard frames with various aperture sizes, placed at a 3 cm distance from the observer's eye (to avoid artificial pupil induced phenomena, e.g., Stiles–Crawford effect of the first kind, etc.) and with the center of the circular opening positioned to match approximately the center of the pupil. Subjects were instructed to fixate at the red fixation light at the back of the Ganzfeld stimulator and to make sure that their head position remained always in such a way to ensure that the fixation light remained at the center of area defined by the border of the aperture at all times. For the RoB and Cone Iso conditions, black cardboard was used to create these aperture frames. The reason was that rod intrusion was small because rods were not (Cone Iso) or only weakly (RoB) stimulated, based on our pilot results. The influence of stray light on the cone-driven response is small because the surrounding retinal area is dark adapted. However, for the WoW condition it was necessary to use white cardboard additionally illuminated with overhead lamps to a mean luminance of 100 cd/m^{2-}, in order to minimize rod intrusion via stray light (for discussion of stray light phenomenon see Aher et al. [27]). ERGs to all stimulus conditions were recorded consecutively within a 1-h recording session; however, the order of stimulus conditions was randomized for each subject. Additionally, within each stimulus condition, the order of presented stimulus sizes was also randomized so as to minimize systematic errors.

Signal analysis

ERG waveforms were analyzed offline, and the amplitudes and implicit peak times were extracted for different ERG components (a-wave, b-wave, i-wave, PhNR and d-wave). The amplitude of the a-wave was measured from the baseline to the first negative trough between 5 and 25 ms after stimulus onset. The amplitude of the b-wave was measured from the trough of the a-wave to the first positive peak (in a window between 24 and 44 ms post-stimulus). The PhNR was measured in two ways: from the baseline to the minimum following the b-wave (labeled PhNR (fB)) within in a window between 50 and 150 ms after stimulus onset and from the preceding b-wave peak (labeled PhNR (fP), same labeling as in Ortiz et al. [29]. Both methods are currently recommended by the PhNR ISCEV extended protocol [13]. After determination of the b-wave and PhNR, the i-wave was identified as the greatest positive deflection on the downward trailing edge of the b-wave (typically with implicit times between 40 and 80 ms), occurring before the PhNR (Fig. 1). A peak-to-trough amplitude of the i-wave was obtained by subtraction of the minimum preceding the i-wave from its maximum.

Data for i-waves for a specific stimulus condition and stimulus size were only analyzed if a minimum of 3 subjects had observable i-waves for that experimental condition. The amplitude of the d-wave was measured from baseline (between 15 and 20 ms after the end of the ON stimulus) to the positive peak 20 to 30 ms after the end of the long flash stimulus.

An estimation of noise for each stimulus condition was obtained by recording ERG signals in the absence of a stimulus, such that the subject was viewing the usual background for each stimulus condition but without a stimulus. The noise recordings were treated identically as the recordings with a stimulus, such that components were measured in the appropriate time windows, namely 5-44 ms ("noise"), and compared with the component data from real recordings ("signal"). Amplitudes and times of a-waves, b-waves, PhNRs and d-waves were discarded when signal-to-noise ratios (SNRs) were less than 2.82 [28].

Estimating relationship with retinal surface area

For each of the seven stimulus sizes, a corresponding retinal area (in mm^2) was utilized for all subsequent data analysis. For the full-field (FF) stimulus size, a total retinal area (in mm^2) was obtained from work by Nagra and colleagues [30], and for stimulus sizes 70° through 20°, retinal areas were calculated based on original work by Drasdo and Fowler [31], using an equation derived by Dacey [32]. Additionally, for areas larger than 30 degrees the area of the optic nerve disc (an average value of 2.69 mm^2) was subtracted from the total retinal area based on calculations by Hoffmann and colleagues [33].

Two approaches were used to establish the relationship between measures (amplitudes, peak times) of ERG components and the retinal surface area. For amplitudes, an exponential fit ("one phase association" in GraphPad Prism) was used:

$$Y = P \times \left(1 - e^{(-k \times x)}\right) \qquad (1)$$

where P is the maximal response (plateau) obtained with "infinitely" large stimuli. Observe that this equation incorporates the requirement that the response is zero ($y = 0$) in the absence of a stimulus (i.e., $x = 0$). For peak times and amplitude ratios, a different exponential fit ("one phase decay" in GraphPad Prism, equation

$$Y = (Y_0 - P) \times e^{(-k \times x)} \qquad (2)$$

where Y_0 is the implicit time or amplitude ratio for very small stimuli. The Plateau (Y_0–P) was constrained to the mean value of the implicit time recorded for the FF size stimulus for the corresponding component. The few cases where the exponential fit was ambiguous or the confidence interval for the k-constant was too wide, a linear regression model was applied.

Statistical analysis

Amplitudes and peak times were averaged within groups. Data were transferred to GraphPad Prism 8 (GraphPad Software Inc., San Diego, CA) for figure creation and statistical evaluation. As part of this model, an extra sum-of-squares F-test was used to calculate difference of slopes.

Results

General trace appearance WoW and RoB

Figure 1 shows averaged ERG responses elicited by the two different types of stimuli (WoW—left plots and RoB—right plots) for the seven different stimulus sizes. In the upper plots, the responses are plotted with the same amplitude scaling (indicated by the scale bars in the upper left corner). In order to identify the different components, in the lower plots the recordings are rescaled to the same b-wave amplitude. In all conditions, the ERG waveforms were generally similar and consisted of an initial brief negative a-wave, followed by a positive b-wave, an unreliable brief i-wave and a gradual negative PhNR. In general, the ERG response amplitudes in both conditions were substantially larger in FF stimuli than to spatially restricted stimuli (i.e., 70° through 20°) and decreased as less retinal surface area was stimulated.

Relationship between amplitudes versus stimulated area

The first level of analysis included an evaluation of relationship between amplitudes vs. stimulated area for both stimulus conditions. The results of this analysis are presented in Fig. 2a, b, Table 1 and
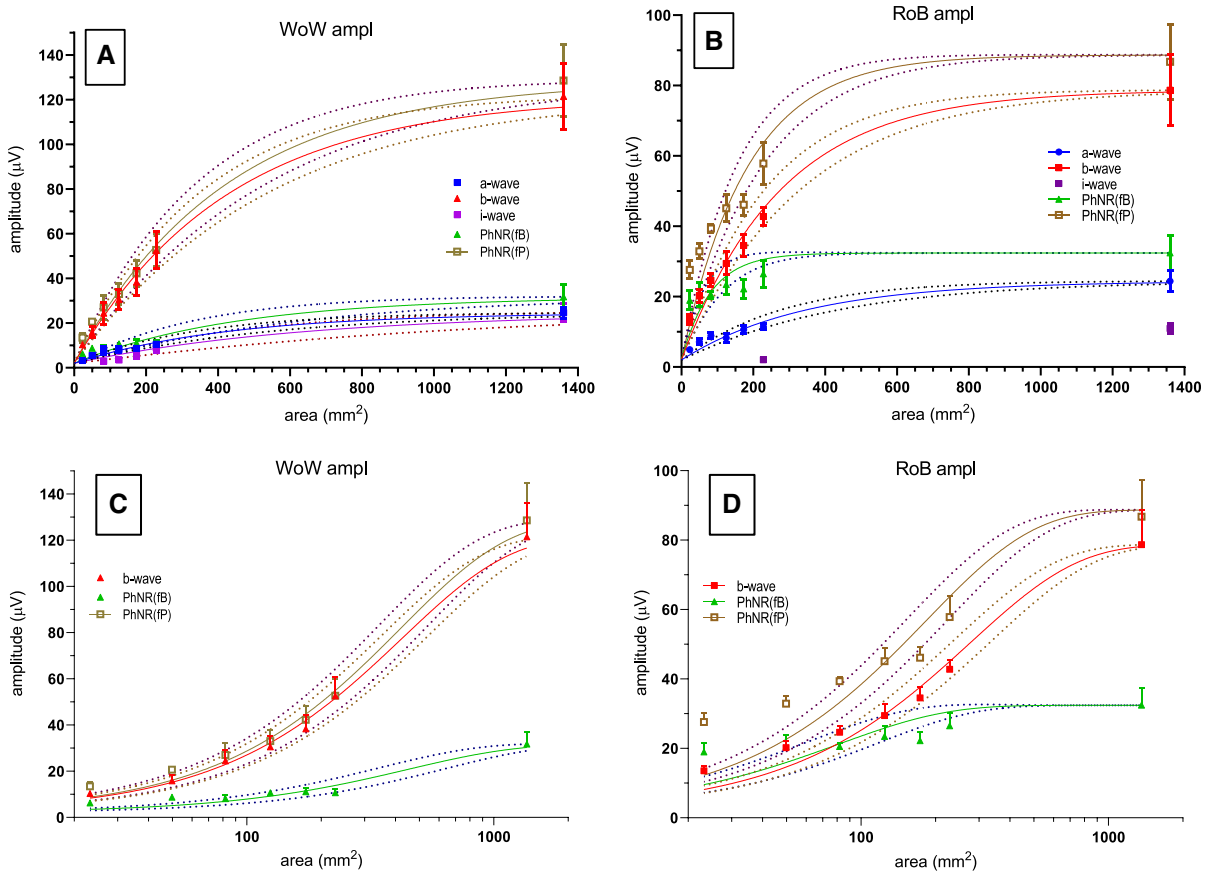
Fig. 2 Relationship between ERG amplitudes and stimulated retinal area for each stimulation condition. **a** ERG amplitudes from the WoW condition; **b** amplitudes for the RoB condition; **c**, **d** amplitudes of select parameters recorded under WoW and RoB conditions plotted on a logarithmic retinal area scale to emphasize the difference in initial rise in amplitude increase (20° to 70°). Averaged amplitudes ($\pm$ SEM) were plotted against the corresponding stimulated retina area. Solid lines indicate an exponential model fit while dashed lines indicate 95% confidence bands (see main text for details)

Table 1 Nonlinear regression (one phase association) of ERG component amplitudes over retinal surface area for WoW and RoB

	WoW		RoB		K-constants' difference
	R^2	K-constant	R^2	K-constant	
a-wave	0.9456	0.0023	0.9252	0.0030	N.S.
b-wave	0.9879	0.0024	0.9453	0.0040	$p = 0.0275$
i-wave	0.8851	0.0017	*N/A*	*N/A*	*N/A*
PhNR (fB)	0.8836	0.0026	− 0.1636	0.0161	$p = 0.0313$*
PhNR (fP)	0.9850	0.0025	0.7702	0.0061	$p = 0.0028$

Units for *k*-constants are 1/mm^2. Unless noted otherwise, the k-constant comparison was done based on a paired two-tailed t-test. The values provided as R^2 and k-constant are the average values of all individual fits; for a full presentation of all individual values, please refer to Supplementary Table 1

*Wilcoxon matched pairs singed rank test

Supplementary Table 1. For all ERG components, amplitudes were largest with the FF stimuli and decreased monotonically with a decrease in stimulus size. As presented in Table 1, the goodness of fit (R^2) of the regression models for all ERG amplitudes was reasonable (0.77–0.99), with the exception of PhNR(fB) (− 0.16–0.88). The k-constant was significantly larger under RoB condition compared to WoW ($p < 0.001$) for the b-wave and PhNR (fits presented on a logarithmic scale in Fig. 2c, d, numeric results in Table 1), while there was no difference between the two k-constants for the a-wave (Table 1, Fig. 3). This indicates that the initial amplitude increase as a function of stimulus size for the b-wave and PhNR is larger for RoB stimuli, even when the maximal RoB response is smaller (b-wave, PhNR(fP)) than or equal (PhNR(fB)) to the maximal WoW response.

There was no statistically significant difference between any of the k-constants of amplitudes vs.

stimulus area under WoW (Table 3). In the RoB condition, the k-constant for PhNR(fB) was significantly larger compared the those of a- or b-wave ($p = 0.0009$ and $p = 0.0219$, respectively), while all other constants were not significantly different ($p > 0.05$).

The frequency of i-wave occurrences depended on stimulus condition. The WoW condition consistently produced i-waves (with the exception of the smallest stimulus size—20°), while the RoB condition generated discernable i-waves only at FF stimulation.

Relationship of amplitude ratios versus stimulated area

The relationship between b-/a-wave amplitude ratio and stimulated retinal area is presented in Fig. 4a). Although the ratio under WoW condition reached a higher plateau, there was no significant difference between the k-constants after fitting with Eq. 2 ($p >$
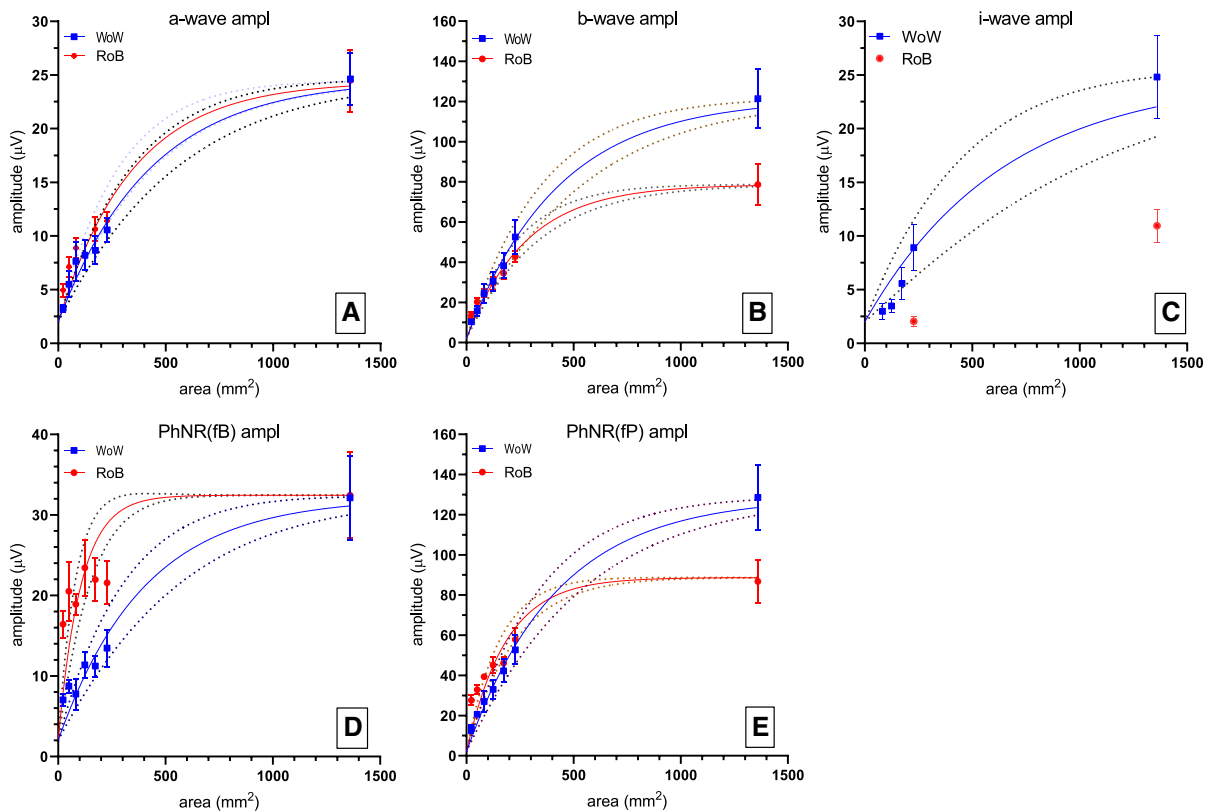

Fig. 3 Relationship between the amplitude of each ERG parameter and stimulated retinal area across two different stimulation conditions (WoW vs. RoB). **a** a-wave amplitudes; **b** b-wave amplitudes; **c** PhNR(fB) amplitudes; **d** PhNR(fP) amplitudes; E) i-wave amplitudes. Averaged amplitudes (± SEM) were plotted against the corresponding stimulated retina area. Solid lines indicate an exponential model fit while dashed lines indicate 95% confidence bands (see main text for details)
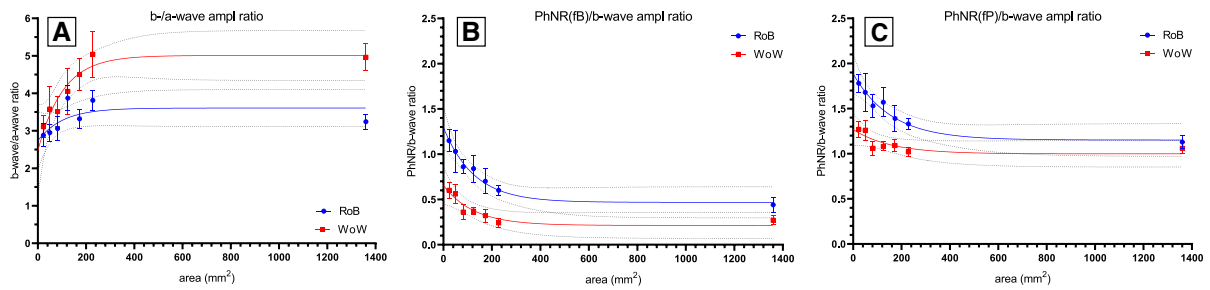
Fig. 4 Relationship between selected ERG amplitude ratios vs. stimulated area. **a** b-/a-wave amplitude ratios; **b** PhNR(fB)/b-wave amplitude ratios; **c** PhNR(fP)/b-wave amplitude ratios. Ratios ($+ 1$ SEM) are plotted as function of stimulated retinal area (mm^2). Solid lines indicate an exponential model fit while dashed lines indicate 95% confidence bands (see main text for details)

0.05, paired t-test). Of note, the goodness of fit was slightly different between the two ratios ($R^2 = 0.5566$ for WoW and 0.3617 for RoB), indicating a more predictable change in the ratio with change in stimulated area for responses recorded under WoW. A comparison between the two conditions was conducted also for the ratio of PhNR(fB) amplitude vs. b-wave amplitude and PhNR(fP) amplitude vs. b-wave amplitude (Fig. 4b and c, respectively, Supplementary Table 2). Here again, despite slightly different appearance, there was no significant difference between the k-constants for either measure ($p > 0.05$, Wilcoxon matched-pairs signed rank test). Of note, an exponential function described relatively well the decline in ratios with eccentricity. Thus, the PhNR(fB)/b-wave ratio the goodness of fit was $R^2 = 0.7888$ (WoW) and 0.6434 (RoB), while the corresponding values for the PhNR(fP)/b-wave ratio were $R^2 = 0.6838$ (WoW) and 0.6169 (RoB).

Relationship of peak times versus stimulated area

Peak times vs. stimulated area were also fitted with Eq. 2, and the results are shown in Fig. 5, Table 2 (and Supplementary Table 3). For both stimulus conditions, the ERG components peak times only changed slightly with stimulus size, although PhNR showed noticeable and well-defined increase in peak time with decreasing stimulated area (Fig. 5).

No significant difference was found between the k-constants of the different ERG parameters under WoW (Table 3). As demonstrated in Supplemental Table 3, for several individual fits, the k-constants for ERG parameters (a-, b- and i-wave) recorded under WoW were estimated to be equal to 0, indicating a linear instead of nonlinear change in the relationship with stimulated retinal area. Therefore, for these parameters, a linear regression fit was conducted also, demonstrating no relationship between timing and stimulated area for the a-wave and a relatively very small change in timing (slope < 0.003 ms/mm^2) for both b- and i-wave. Slight non-linearly for timing vs

Table 2 Nonlinear regression (one phase decay) of peak times over retinal surface area for WoW and RoB

	WOW		ROB		K-constants' difference
	R^2	K-constant	R^2	K-constant	
a-wave	0.4654	0.0361	0.4982	0.0207	N.S.
b-wave	0.6439	0.0029	0.7741	0.0304	$p = 0.0313$
i-wave	0.7765	0.0050	N/A	N/A	
PhNR	0.6986	0.0067	0.6582	0.0054	N.S.

Units for k-constants are 1/mm^2. The k-constant comparison was done based on Wilcoxon matched pairs singed rank test. The values provided as R^2 and k-constant are the average values of all individual fits; for a full presentation of all individual values, please refer to Supplementary Table 3

Table 3 Differences between k-constants for amplitudes and peak times recorded under WoW or RoB condition

	Amplitudes WoW					Peak times WoW		
	b-wave	PhNR(fB)	PhNR(fP)	I-wave		b-wave	PhNR	i-wave
a-wave	N.S.	N.S.	N.S.	N.S.	a-wave	$p = 0.0152$	N.S.	p = 0.0311
b-wave		N.S.	N.S.	N.S.	b-wave		N.S.	N.S.
PhNR(fB)			N.S.	N.S.	PhNR			N.S.
PhNR(fP)				N.S.				
	Amplitudes RoB					Peak times RoB		
	b-wave	PhNR(fB)	PhNR(fP)			b-wave	PhNR	
a-wave	N.S.	p = 0.0009	N.S.		a-wave	N.S.	N.S.	
b-wave		p = 0.0219	N.S.		b-wave		N.S.	
PhNR(fB)			N.S.					

As most parameters were not normally distributed, the results (adjusted p-values) from Dunn's multiple comparisons tests are shown
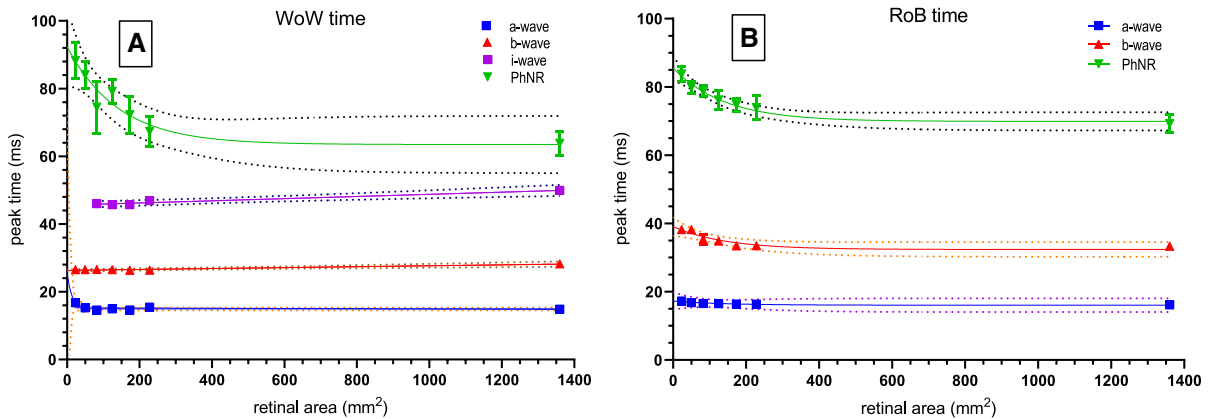

Fig. 5 Relationship between ERG peak times and stimulated retinal area across two different stimulation conditions (WoW vs. RoB). **a** ERG peak times from the WoW condition; **b** peak times for the RoB condition. Averaged peak times (± SEM) were plotted against the corresponding stimulated retina area. Solid lines indicate an exponential model fit while dashed lines indicate 95% confidence bands (see main text for details)

stimulated area of ERG parameters under RoB was observed (Table 3), although here also in some subjects the k-constants were estimated to be equal to 0 and the inter-individual variation in k-constants was significant (Supplementary Table 3), suggesting that the results should be interpreted with caution. As under WoW, no significant difference between individual k-constants was observed under RoB (Table 3).

Interestingly, the peak times of the PhNR decreased more strongly with increasing stimulus size than the other components, indicating that the generators of the PhNR show a stronger contrast gain mechanism in which the responses occur earlier as the response

amplitude increases. This is known to occur in the responses of magnocellular retinal ganglion cells [34, 35].

Cone isolating stimuli

Although we recorded ERG signals under cone isolating long-flash stimulus conditions within the same recording session as under the WoW and RoB short-flash stimulus conditions, we report them separately. A direct comparison between responses generated by the two type of stimuli is not straightforward because components that are separated in long-flash

Fig. 6 Averaged ERG traces (±SEM) recorded from six subjects for the seven different stimulus configurations with cone isolating stimuli (FF and 70°, 60°, 50°, 40°, 30° and 20° diameter) are presented. **a** ERG responses presented as absolute amplitudes; **b** same ERG responses as in **a** with equalized b-wave amplitudes. Dotted horizontal lines in each trace represent the baseline. The thick dotted vertical lines indicate the onset and offset of flash stimulus. The thin dotted vertical lines indicate the time of each wave's peak occurrence for the FF stimulus (top row), allowing for comparison with smaller stimulus sizes (rows below). The nomenclature of the ERG components is also presented for FF, including the a-wave, b-wave, i-wave, PhNR, d-wave and i(d)-wave
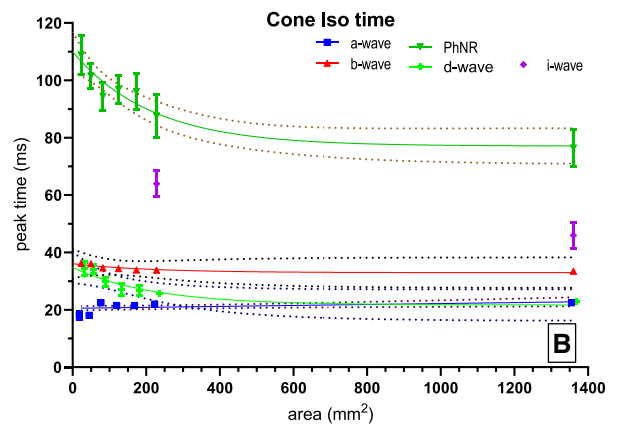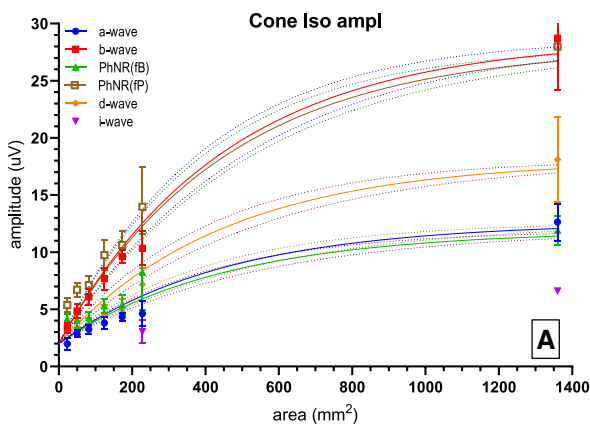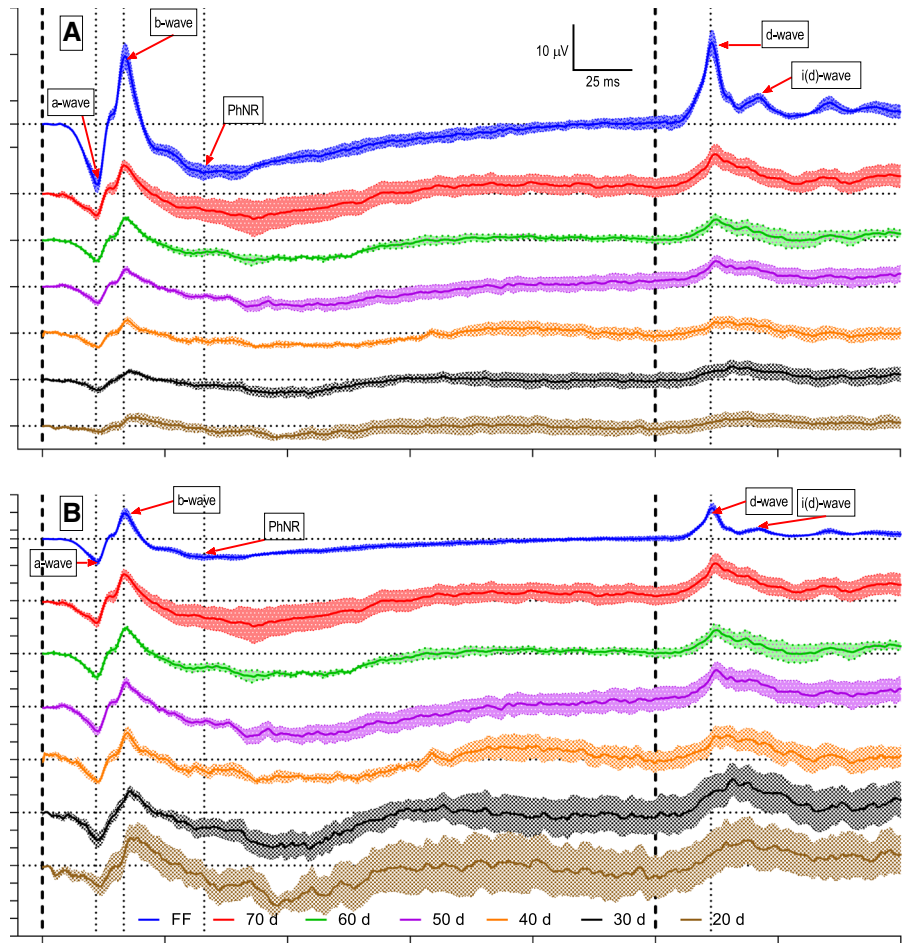

Fig. 7 Relationship between ERG amplitudes and peak times vs. stimulated retinal area for cone isolating stimuli. **a** Amplitudes versus stimulated area; **b** peak times vs. stimulated area. Averaged amplitudes or peak times (± SEM) were plotted against the corresponding stimulated retina area. Solid lines indicate an exponential model fit while dashed lines indicate 95% confidence bands (see main text for details)

Table 4 Nonlinear regression (one phase association or one phase decay) of amplitudes or peak times over retinal surface area for Cone Iso

	Cone Iso amplitudes		Cone Iso peak times	
	R^2	K-constant	R^2	K-constant
a-wave	0.9316	0.0017	0.6857	0.0350
b-wave	0.9718	0.0022	0.6378	0.0134
d-wave	0.9441	0.0018	0.8503	0.0216
PhNR (fB)	0.6904	0.0036	0.8331	0.0048
PhNR (fP)	0.9525	0.0027		

Units for k-constants are 1/mm^2. The values provided as R^2 and k-constant are the average values of all individual fits; for a full presentation of all individual values, please refer to Supplementary Tables 4 and 5

conditions merge in the responses to short flashes. Figure 6 shows averaged ERG responses elicited by L− + M-cone isolating stimuli for the seven different stimulus sizes. Again, the scaling of the lower plots is normalized to the amplitudes of the b-wave, so that the different components can be better recognized for all stimulus sizes. As with responses recorded under WoW or RoB, here also a similarity between the waveforms obtained across different stimulus sizes was noticeable. All traces showed the presence of an a-wave, b-wave, PhNR and a d-wave. Additionally, a secondary peak after the d-wave, labeled "i(d)-wave" was noticeable in most traces, although the signal-to-noise ratio for this component passed our criterion only for FF and 70 deg stimulus.

The amplitude and peak time data of the components obtained under Cone Iso stimuli and their relationship with the size of the stimulated area are presented in Fig. 7, while the results of model fits are

summarized in Table 4. In general, exponential fits described the relationship between amplitudes or peak times and stimulated area well. There was no significant difference between the four k-constants of amplitude components, while a couple of significant differences were noted between the constants describing peak times (Table 5).

The relationship between amplitude ratios vs. stimulated area of ERG components obtained under Cone Iso stimuli is presented in Fig. 8, while the results of the nonlinear fits are presented in Supplementary Table 6. In contrast with the relationship between amplitudes recorded under Cone Iso stimuli and size of the stimulated area, most amplitude ratios showed an irregular pattern when plotted against size of stimulated area, and the goodness of fit of relationship amplitude ratio vs. area (R^2) was considerably lower and the coefficient of variation for the k-constants was quite high (>67%, Supplementary Table 6), indicating considerable individual irregularity and substantial inter-individual variability.

Discussion

The goal of this ERG study was twofold. First, we wanted to elucidate trends in photopic ERG parameters across a broad range of stimulated retinal areas. Second, we wanted to compare the relationships between ERG parameters and stimulated areas for two different stimulus conditions where the stimulus was a brief flash and to see also how this relationship holds for responses recorded under an L- + M-cone isolating stimulus (long duration stimulus). Our results indicate that, in most cases, a simple exponential fit (either increasing or decreasing with size of stimulated

Table 5 Differences between k-constants for amplitudes and peak times recorded under Cone Iso condition

	Amplitudes Cone Iso					Peak times Cone Iso		
	b-wave	PhNR(fB)	PhNR(fP)	d-wave		b-wave	PhNR	d-wave
a-wave	N.S.	N.S.	N.S.	N.S.	a-wave	$p = 0.0437$	$p = 0.0105$	N.S.
b-wave		N.S.	N.S.	N.S.	b-wave		N.S.	N.S.
PhNR(fB)			N.S.	N.S.	PhNR			N.S.
PhNR(fP)				N.S.				

As most parameters were not normally distributed, the results (adjusted p-values) from Dunn's multiple comparisons tests are shown
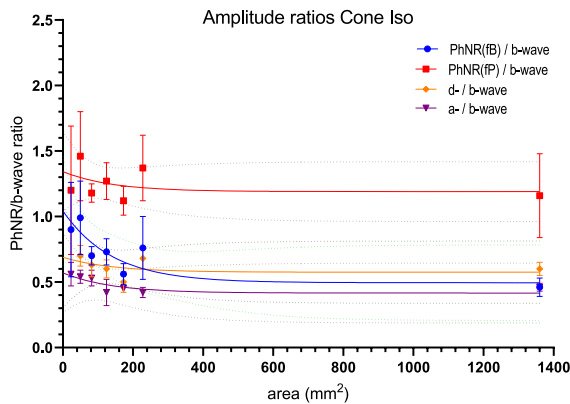
Fig. 8 Selected ERG amplitude ratios vs. stimulated area under cone-isolating stimuli condition. Ratios (+ 1 SEM) are plotted as function of stimulated retinal area (mm²). Solid lines indicate an exponential model fit while dashed lines indicate 95% confidence bands (see main text for details)

retina) with a plateau described the relationship between stimulus parameters and size of stimulated area well.

Exponential fits of the major ERG components' data (a-, b-wave, PhNR)

As we discussed before [36, 37], the nonlinear exponential function reflects probably the fact that the retina is spatially not homogeneous. If the retina were homogeneous, the relationship between amplitude and stimulus area is expected to be linear. However, cell densities decrease with increasing eccentricity. Furthermore, additional factors such as changes in pigment concentration and convergence of photoreceptors to bipolar cells and of bipolar cells to ganglion cells may influence the relationship of amplitude vs. stimulus size. For example, the inverse relationship between the PhNR vs b-wave ratio and stimulus area may reflect an increasing signal convergence with increasing retinal eccentricity (i.e., more bipolar cells are connected to a ganglion cell).

Despite considerable differences in absolute amplitude, the k-constants for a- and b-waves under all stimulating conditions were similar (range 0.0024–0.0038, Tables 1 and 3), although the constants under RoB were higher compared to ones calculated under WoW. These findings corroborate with anatomical data. Specifically, it has been demonstrated that cone photoreceptors follow a

predictable distribution within the eccentricity range used in the current study [36, 37] and that distribution is reflected in ERGs that are driven by activity of the luminance retinal pathway [38–41]. Few studies have shown similar predictable distribution of bipolar cells (believed to be involved directly in the generation of the a-wave and b-wave) in New World primates [21], and more recently in humans [42].

The b-/a-wave ratio increased with increasing stimulus area. This may reflect stronger decrease in cone photoreceptor than bipolar cell density with increasing eccentricity. Indeed, from the data provided by Grünert and Martin [43] we estimated that cone density decreases by a factor 40 – 50 from fovea to 10 mm eccentricity (equivalent to an 80 deg diameter) stimulus eccentricity, whereas cone bipolar cell density decreases by a factor of 9. Of note, the b-/a-wave ratios had similar k-constants for responses recorded under both WoW and RoB, a finding that warrants further investigation.

The PhNR/b-wave ratios decrease with increasing stimulus size, indicating that the generators of the PhNR decrease more strongly with increasing stimulus size compared to the generators of the b-wave. This observation confirms previous findings by Kinoshita et al. of an increased PhNR/b-wave ratio in cynomolgus monkeys for focal macular ERG (15 deg) vs FF stimulus under RoB condition [20]. Assuming that the PhNR originates in activity of the retinal ganglion cells and the b-wave reflects (ON-) bipolar cell activity, these results suggest that, within the spatially restricted central area used in this study (20 to 70 deg), there is an increasing convergence of cone-driven signals with increasing eccentricity [21].

Although it may be tempting to tests the correlations between magnitude of retinal responses and underlying number of stimulated retinal neurons, several limitations restrict the usefulness of this approach. Particularly for the RoB conditions, S-, M- and L-cone are stimulated differently, and this distorts the relationship between stimulated cone numbers and the post-receptor pathways. This distortion becomes more complicated when one additionally considers that the L/M ratios change with retinal eccentricity. Furthermore, the cone input strengths to post-receptoral pathways are not considered. The magnocellular luminance channel has L- and M-cone strengths that probably are proportional to the number of cones. The parvocellular red–green chromatic channel readjusts

the L and M-cone signal strengths to be about equal. As a result, the L/M ratio is about 1 in the midget pathway. Furthermore, factors such as the relative numbers of magno- to parvocellular cells, the possible change with retinal eccentricity, the influence of, e.g., the koniocellular pathway and the unknown relationship between pathway activity and ERG response should be considered.

PhNR amplitude and effect of method of measurement

The PhNR was of particular interest in the present study because it reflects retinal ganglion cell (RGC) activity, a clinically significant cell population in glaucoma and other ocular pathologies [14, 44]. The stimulus conditions that we used for full-field stimulation under RoB conditions matched those recommended by the ISCEV extended protocol for PhNR measurement well, while the stimulus conditions for full-field WoW matched those of the ISCEV standard ERG protocol. Therefore, the comparison between the two conditions including full-field stimulation and spatially restricted stimuli could be of potential interest for clinical application. However, different ways of PhNR amplitude measurement (e.g., from the isoelectric baseline or from the preceding b-wave peak) could have an effect on relationships between PhNR and other ERG parameters, both from theoretical point of view [13], as well as in clinical applications [29]. In our experience, the exponential fit was poorer for the PhNR(fB) than for the PhNR(fP) under all three stimulation conditions. Interestingly, the k-constants did not differ significantly between PhNR(fB) and PhNR(fP) under all three conditions. Furthermore, for both PhNR(fB) and PhNR(fP), the k-constants were the largest under RoB. It has to be noted, however, that the two recording conditions (WoW vs. RoB), while similar in stimulus strength, differed in background luminance (25 cd/m² vs. 10 cd/m²) and this could have influenced the different pattern of change in ratio of amplitude vs. stimulated area.

The shapes of the fits to the PhNR(fP)/b-wave ratio and the PhNR(fB)/b-wave ratio were very similar, and there was no difference in k-constants between WoW and RoB conditions (Fig. 4). This indicates that the generators of the PhNR and the b-wave are identical for WoW and RoB conditions.

ERG components' time trends

The peak times of the individual ERG components under each condition were fairly stable across different stimulus sizes. This general finding indicates that the basic mechanisms which determine the rate of signal transduction do not vary significantly with retinal eccentricity. For example, the change in mean a-wave peak time from the largest stimulus (full-field) to the smallest stimulus (20 deg) was an increase of less than 2 ms under both stimulus conditions, which may be considered too small to have a practical significance.

In contrast, the difference for PhNR peak time was substantial (an increase of 10.8 ms under RoB and 21.6 ms under WoW) emphasizing its different origin and unique properties. As mentioned above, ganglion cells belonging to the magnocellular pathway, which are expected to respond particularly strongly to the applied stimuli, respond earlier as response amplitude increases. This effect is thought to be caused by a control gain control mechanism [35, 45]. The change of the PhNR peak time possibly reflects the contrast gain control. However, the PhNR implicit times of 80 ms and more are larger than the times to maximal response in magnocellular ganglion cells to flashed stimuli [46]. Thus, the PhNR may originate in spiking activity of the ganglion cells [47] but is not a direct expression thereof.

Importantly, under both conditions an exponential fit described the relationship with size of stimulated retina well (which was true also under Cone Iso conditions) and there was no difference in the k-constants (Table 2). A similar increase in PhNR peak time with diminishing stimulus size under ROB conditions was found recently by Morny et al. [48], although they used lower stimulus luminance (0.28 cd.s/m²) and higher stimulation rate (4 Hz).

An interesting phenomenon in our study was the change in i-wave peak time vs. area under WoW which showed a slightly positive, but significantly different from zero linear slope within its recordable range (full field to 40 deg). Furthermore, this slope was significantly different from the slope of the b-wave (p=0.0019). This finding may support the hypothesis of the i-wave as a component with a generation source relatively independent from the other ERG components.
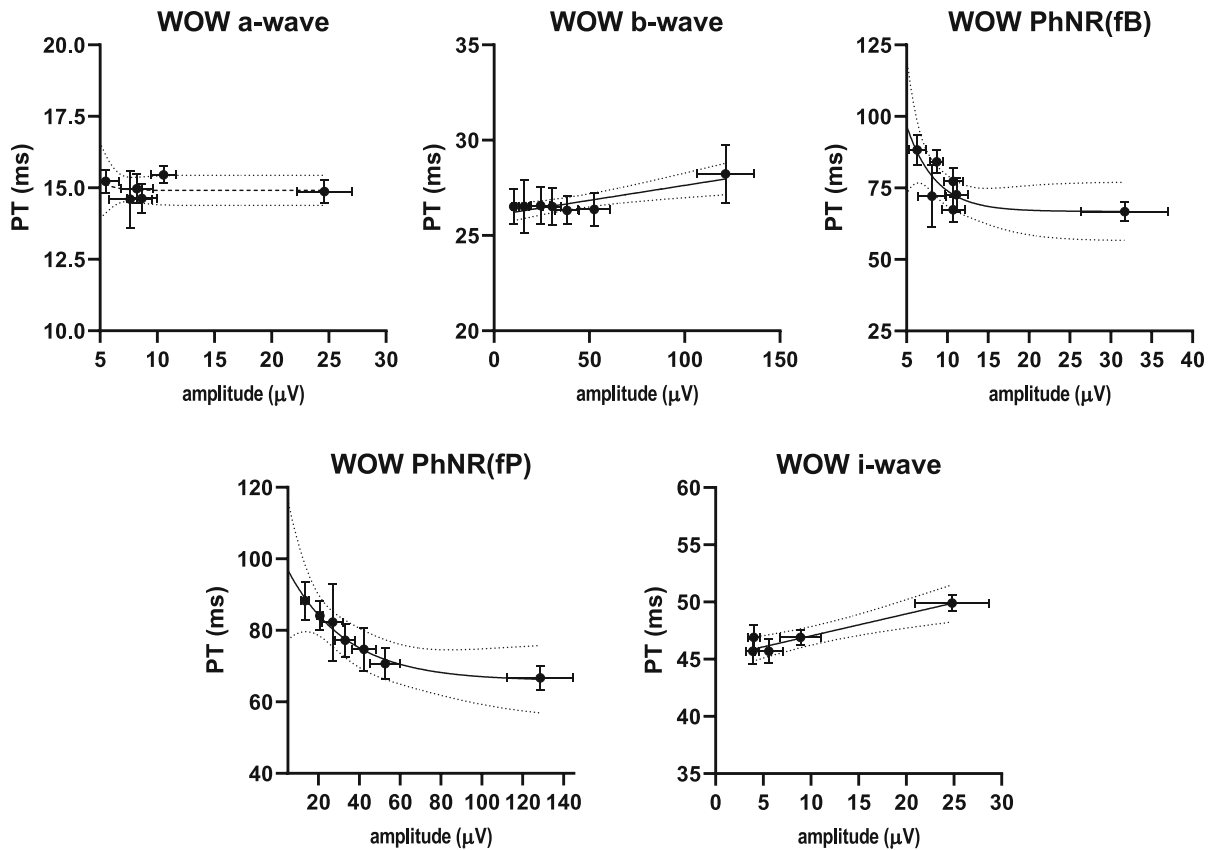
Fig. 9 Relationship between peak time and amplitude for ERG parameters recorded under WoW stimuli. **a** a-wave; **b** b-wave; **c** PhNR(fb); **d** PhNR(fP); **e** i-wave. For a-wave, PhNR(fB) and PhNR(fP) an exponential plot fitted the data well and is presented; for b-wave and i-wave, a linear plot provided a better fit and is shown; dashed lines indicate 95% confidence bands (see main text for details)

Cone isolating stimuli

Although there were some similarities between the results obtained under WoW or RoB stimulation with brief flashes, on one hand, and under Cone Iso stimulation with long flashes on the other hand, it may not be entirely appropriate to compare the stimulus size effects of long duration and brief flashes. The light onset and offset components overlap in the brief flash responses but are separated in the long-flash response [49, 50]. Furthermore, PhNR responses overlap in the brief flash response [51].

With these limitations in mind, it has to be noted that the overall shape of the response was similar between the main ERG parameters recorded with brief flashes and with long flashes. Thus, the average amplitude fits demonstrated similar and excellent goodness of fit (above 0.93) for a- and b-waves for

brief flashes and a-, b- and d-wave recorded with long flashes (Tables 1 and 4). Similarly, under all three conditions, the PhNR(fB) amplitude goodness of fit was considerably worse compared to that of a- and b-waves, while the PhNR(fP) fits were similar to that of the b-wave. Furthermore, the k-constants were similar for a- and b-wave amplitudes under all three conditions, while the PhNR k-constants were similar in WoW and Cone Iso, but larger in RoB. As a general observation, the relationships between timing and stimulated area were more variable between the three conditions. It has to be emphasized that our stimulus conditions were quite different from most other methods used in the literature and a direct comparison in terms of amplitude ratios vs. stimulated area may not be appropriate. This may explain why Kondo et al found an increase in d-/b-wave amplitude ratio with

eccentricity using on-off photopic mfERG [52], in variance with our observations.

Correlation between peak times and amplitudes

When evaluating relationship of peak times with stimulated area, it is worth noting that peak times are not completely independent and are correlated with amplitude, sometimes in a different way for each ERG component. To illustrate that, peak times are plotted as a function of the response amplitude for the WoW condition in Fig. 9. As shown in the figure, for three of the components (a-wave, PhNR(fB) and PhNR(fP)), the correlation between amplitude and peak time can be described relatively well with an exponential fit (R^2 = 0.8469, 0.6360, 0.8854, respectively) while for two of them (b-wave and i-wave), a linear fit describes the correlation much better (R^2 = 0.7769, 0.9731, respectively).

Future directions

Surprisingly, strong linearity was observed in the relationship between b-wave amplitude and size of stimulated retinal area within the central 20 to 70° for WoW (R^2 = 0.9911, slope=0.1981 μV/mm^2, data not shown separately). This observation, together with the observation that b-wave peak time did not change under the same conditions ($p > 0.05$, slope not significantly different from zero; data not shown separately), suggests the possibility that this set of spatially restricted stimuli could be used to test the function of the central retina in a novel way by applying spatially restricted stimuli under clinical conditions. Currently, the most common way of testing the function of the central retina under photopic conditions is with multifocal ERG [53]. However, although the multifocal ERG provides a topographical localization of the responses within the central retina, its interpretation and cellular origin are less certain compared to that of full-field (flash) ERG. Only when the m-sequence of the mfERG is slowed down (at least 5 times), the shape of the mfERG individual waveforms matches the shape of the waveform of the full-field flash ERG [54], which makes it difficult to use clinically. Therefore, a spatially restricted flash ERG protocol could be a useful addition to the standard flash ERG protocol and could increase its sensitivity to functional changes in the central retina, especially in

diseases affecting the paramacular region, a possibility that will be explored further.

Limitations

Certain limitations of this study include the relatively low number of human subjects tested on, as well as the similar ethnic background of all six subjects. However, the data were quite consistent and we are confident that the effects described here are representative for the normal human visual system. Another difficulty of ERG recordings utilizing smaller stimulus sizes is that background noise begins to approach absolute values close to signal amplitudes. We experimented with using an increased number of trials for smaller stimuli and found that the signal-to-noise ratio (SNR) improves with increased number of averages. Therefore, trends in response amplitude with decreasing stimulus size are indeed due to change in the signal and not simply because of increased noise contribution. The figures with the normalized original responses (Figs. 1 and 6; lower plots) clearly show that all components could be clearly identified, although the SNRs was still smaller at smaller stimulus sizes compared to the FF responses.

Although detailed studies exploring the topographical distribution of ON- and OFF-bipolar pathways in the human macular and paramacular regions are lacking, data from non-human primates indicate that a difference in the number of OFF-bipolar cells associated with the S-cone pathway vs. the L+M-cone pathway may exist in favor of the latter. Such a difference may have an influence in the responses recorded under the conditions used in the present study, especially when comparing responses rec0rded under WoW vs. RoB. The exact nature of this influence is uncertain and will be subject of future studies.

Several anatomical and functional variables change within the eccentricity range tested in the current study. The list of such factors includes, but is not limited to cone densities, densities of connected bipolar and ganglion cells, convergence factors within the retinal pathways, receptive field size, On-Off color opponent disbalance, axonal fiber diameter, flicker fusion frequency, etc. Some contribution from the Stiles–Crawford effect at lower retinal eccentricities, although minimal, cannot be completely ruled out too. It is impossible at this preliminary stage of our work to

make an informed guess as to which of these factors are truly relevant and how this relevancy would be ranked. Future studies would be designed and conducted to address these questions.

Conclusion

This investigational study characterizes ERG responses to three different light stimuli across a wide range of retinal area sizes in normal human subjects. By elucidating how varied stimulus conditions and sizes affect the electrophysiological behavior of individual ERG components, we hope to contribute toward improving the sensitivity and utility of functional ERG assessments of retinal health. Further work is warranted to determine how specific retinal disease states may cause deviation from our initial physiological results, and the ways in which targeted central retina stimulation can be applied clinically.

Compliance with ethical standrds

Conflict of interest All authors certify that they have no affiliations with or involvement in any organization or entity with any financial interest (such as honoraria; educational grants; participation in speakers' bureaus; membership, employment, consultancies, stock ownership, or other equity interest; and expert testimony or patent-licensing arrangements), or non-financial interest (such as personal or professional relationships, affiliations, knowledge or beliefs) in the subject matter or materials discussed in this manuscript.

Ethical approval All procedures performed in studies involving human participants were in accordance with the ethical standards of the University Hospital Erlangen and University of South Florida and with the 1964 Helsinki Declaration and its later amendments or comparable ethical standards.

Informed consent Informed consent was obtained from all individual participants included in the study.

References

1. Robson JG, Saszik SM, Ahmed J et al (2003) Rod and cone contributions to the a-wave of the electroretinogram of the macaque. J Physiol 547:509–530. https://doi.org/10.1113/jphysiol.2002.030304
2. Bush RA, Sieving PA (1994) A proximal retinal component in the primate photopic ERG a-wave. Invest Ophthalmol Vis Sci 35:635–645
3. Ueno S, Kondo M, Niwa Y et al (2004) Luminance dependence of neural components that underlies the primate photopic electroretinogram. Invest Ophthalmol Vis Sci 45:1033–1040. https://doi.org/10.1167/iovs.03-0657
4. Dong CJ, Hare WA (2000) Contribution to the kinetics and amplitude of the electroretinogram b-wave by third-order retinal neurons in the rabbit retina. Vision Res 40:579–589. https://doi.org/10.1016/s0042-6989(99)00203-5
5. Rufiange M, Rousseau S, Dembinska O et al (2002) Cone-dominated ERG luminance-response function: the Photopic Hill revisited. Documenta Ophthalmol Adv Ophthalmol 104:231–248
6. Rosolen SG, Rigaudière F, LeGargasson J-F et al (2004) Comparing the photopic ERG i-wave in different species. Veterinary Ophthalmol 7:189–192. https://doi.org/10.1111/j.1463-5224.2004.04022.x
7. Rangaswamy NV, Frishman LJ, Dorotheo EU et al (2004) Photopic ERGs in patients with optic neuropathies: comparison with primate ERGs after pharmacologic blockade of inner retina. Invest Ophthalmol Vis Sci 45:3827–3837. https://doi.org/10.1167/iovs.04-0458
8. Viswanathan S, Frishman LJ, Robson JG et al (2001) The photopic negative response of the flash electroretinogram in primary open angle glaucoma. Invest Ophthalmol Vis Sci 42:514–522
9. Colotto A, Falsini B, Salgarello T et al (2000) Photopic negative response of the human ERG: losses associated with glaucomatous damage. Invest Ophthalmol Vis Sci 41:2205–2211
10. Gotoh Y, Machida S, Tazawa Y (2004) Selective loss of the photopic negative response in patients with opticnerve atrophy. Arch Ophthalmol 122:341–346. https://doi.org/10.1001/archopht.122.3.341
11. McCulloch DL, Marmor MF, Brigell MG et al (2015) ISCEV standard for full-field electroretinography (2015 update). Doc Ophthalmol 130:1–12. https://doi.org/10.1007/s10633-014-9473-7
12. Rangaswamy NV, Shirato S, Kaneko M et al (2007) Effects of spectral characteristics of ganzfeld stimuli on the photopic negative response (PhNR) of the ERG. Invest Ophthalmol Vis Sci 48:4818–4828. https://doi.org/10.1167/iovs.07-0218
13. Frishman L, Sustar M, Kremers J et al (2018) ISCEV extended protocol for the photopic negative response (PhNR) of the full-field electroretinogram. Doc Ophthalmol 136:207–211. https://doi.org/10.1007/s10633-018-9638-x
14. Kremers J, Jertila M, Link B et al (2012) Spectral characteristics of the PhNR in the full-field flash electroretinogram of normals and glaucoma patients. Doc Ophthalmol 124:79–90. https://doi.org/10.1007/s10633-011-9304-z

15. Tsai TI, Jacob MM, McKeefry D et al (2016) Spatial properties of L- and M-cone driven incremental (On-) and decremental (Off-) electroretinograms: evidence for the involvement of multiple post-receptoral mechanisms. J Opt Soc Am A Opt Image Sci Vis 33:A1–A11. https://doi.org/10.1364/josaa.33.0000a1

16. de Graaf B, Wertheim AH (1988) The perception of object motion during smooth pursuit eye movements: adjacency is not a factor contributing to the Filehne illusion. Vision Res 28:497–502. https://doi.org/10.1016/0042-6989(88)90172-1

17. Miyake Y (1998) Focal macular electroretinography. Nagoya J Med Sci 61:79–84

18. Machida S, Toba Y, Ohtaki A et al (2008) Photopic negative response of focal electoretinograms in glaucomatous eyes. Invest Ophthalmol Vis Sci 49:5636–5644. https://doi.org/10.1167/iovs.08-1946

19. Machida S, Tamada K, Oikawa T et al (2010) Sensitivity and specificity of photopic negative response of focal electoretinogram to detect glaucomatous eyes. Br J Ophthalmol 94:202–208. https://doi.org/10.1136/bjo.2009.161166

20. Kinoshita J, Takada S, Iwata N et al (2016) Comparison of photopic negative response (PhNR) between focal macular and full-field electroretinograms in monkeys. Documenta Ophthalmologica. Adv Ophthalmol 132:177–187. https://doi.org/10.1007/s10633-016-9538-x

21. Martin PR, Grünert U (1992) Spatial density and immunoreactivity of bipolar cells in the macaque monkey retina. J Compar Neurol 323:269–287. https://doi.org/10.1002/cne.903230210

22. Dawson WW, Trick GL, Litzkow CA (1979) Improved electrode for electroretinography. Invest Ophthalmol Vis Sci 18:988–991

23. Kremers J (2003) The assessment of L- and M-cone specific electroretinographical signals in the normal and abnormal human retina. Prog Retinal Eye Res 22:579–605

24. Estévez O, Spekreijse H (1982) The "silent substitution" method in visual research. Vision Res 22:681–691. https://doi.org/10.1016/0042-6989(82)90104-3

25. Donner KO, Rushton WA (1959) Retinal stimulation by light substitution. J Physiol 149:288–302. https://doi.org/10.1113/jphysiol.1959.sp006340

26. Shapiro AG, Pokorny J, Smith VC (1996) Cone-rod receptor spaces with illustrations that use CRT phosphor and light-emitting-diode spectra. J Opt Soc Am A Opt Image Sci Vision 13:2319–2328

27. Aher AJ, McKeefry DJ, Parry NRA et al (2018) Rod- versus cone-driven ERGs at different stimulus sizes in normal subjects and retinitis pigmentosa patients. Documenta Ophthalmologica. Adv Ophthalmol 136:27–43. https://doi.org/10.1007/s10633-017-9619-5

28. Meigen T, Bach M (1999) On the statistical significance of electrophysiological steady-state responses. Documenta Ophthalmologica. Adv Ophthalmol 98:207–232

29. Ortiz G, Drucker D, Hyde C et al (2020) The photopic negative response of the Light-adapted 3.0 ERG in clinical settings. Doc Ophthalmol 140:115–128. https://doi.org/10.1007/s10633-019-09723-5

30. Nagra M, Gilmartin B, Thai NJ et al (2017) Determination of retinal surface area. J Anat 231:319–324. https://doi.org/10.1111/joa.12641

31. Drasdo N, Fowler CW (1974) Non-linear projection of the retinal image in a wide-angle schematic eye. Br J Ophthalmol 58:709–714. https://doi.org/10.1136/bjo.58.8.709

32. Dacey DM (1993) The mosaic of midget ganglion cells in the human retina. J Neurosci 13:5334–5355

33. Hoffmann EM, Zangwill LM, Crowston JG et al (2007) Optic disk size and glaucoma. Survey Ophthalmol 52:32–49. https://doi.org/10.1016/j.survophthal.2006

34. Victor JD, Shapley RM (1979) The nonlinear pathway of Y ganglion cells in the cat retina. J Gen Physiol 74:671–689. https://doi.org/10.1085/jgp.74.6.671

35. Yeh T, Lee BB, Kremers J (1995) Temporal response of ganglion cells of the macaque retina to cone-specific modulation. J Opt Soc Am A Opt Image Sci Vis 12:456–464. https://doi.org/10.1364/josaa.12.000456

36. Curcio CA, Allen KA (1990) Topography of ganglion cells in human retina. J Comp Neurol 300:5–25. https://doi.org/10.1002/cne.903000103

37. Curcio CA, Millican CL, Allen KA et al (1993) Aging of the human photoreceptor mosaic: evidence for selective vulnerability of rods in central retina. Invest Ophthalmol Vis Sci 34:3278–3296

38. Jacob MM, Pangeni G, Gomes BD et al (2015) The spatial properties of L- and M-cone inputs to electroretinograms that reflect different types of post-receptoral processing. PLoS ONE 10:e0121218. https://doi.org/10.1371/journal.pone.0121218

39. Murray IJ, Parry NR, Kremers J et al (2004) Photoreceptor topography and cone-specific electroretinograms. Vis Neurosci 21:231–235. https://doi.org/10.1017/s0952523804213268

40. Rodrigues AR, FilhoMda S, Silveira LC et al (2010) Spatial distributions of on- and off-responses determined with the multifocal ERG. Doc Ophthalmol 120:145–158. https://doi.org/10.1007/s10633-009-9205-6

41. Martins CMG, Tsai T, Barboni MTS et al (2016) The influence of stimulus size on heterochromatic modulation electroretinograms. J Vision 16:13. https://doi.org/10.1167/16.8.13

42. Masri R (2019) Neurons of the primate retina: a qualitative and quantitative analysis, in save sight institute and discipline of ophthalmology. University of Sydney, Sydney

43. Grunert U, Martin PR (2020) Cell types and cell circuits in human and non-human primate retina. Prog Retin Eye Res. https://doi.org/10.1016/j.preteyeres.2020.100844

44. Porciatti V (2015) Electrophysiological assessment of retinal ganglion cell function. Exp Eye Res 141:164–170. https://doi.org/10.1016/j.exer.2015.05.008

45. Shapley RM, Victor JD (1978) The effect of contrast on the transfer properties of cat retinal ganglion cells. J Physiol 285:275–298. https://doi.org/10.1113/jphysiol.1978.sp012571

46. Lee BB, Wehrhahn C, Westheimer G et al (1995) The spatial precision of macaque ganglion cell responses in relation to vernier acuity of human observers. Vision Res 35:2743–2758. https://doi.org/10.1016/0042-6989(95)00015-r

47. Viswanathan S, Frishman LJ, Robson JG et al (1999) The photopic negative response of the macaque electroretinogram: reduction by experimental glaucoma. Invest Ophthalmol Vis Sci 40:1124–1136

48. Morny EKA, Patel K, Votruba M et al (2019) The relationship between the photopic negative response and retinal ganglion cell topography. Invest Ophthalmol Vis Sci 60:1879–1887. https://doi.org/10.1167/iovs.18-25272

49. Kondo M, Piao CH, Tanikawa A et al (2000) Amplitude decrease of photopic ERG b-wave at higher stimulus intensities in humans. Jpn J Ophthalmol 44:20–28. https://doi.org/10.1016/s0021-5155(99)00172-0

50. Sustar M, Hawlina M, Brecelj J (2006) ON- and OFF-response of the photopic electroretinogram in relation to stimulus characteristics. Documenta Ophthalmologica. Adv Ophthalmol 113:43–52. https://doi.org/10.1007/s10633-006-9013-1

51. Kondo M, Kurimoto Y, Sakai T et al (2008) Recording focal macular photopic negative response (PhNR) from monkeys.

Invest Ophthalmol Vis Sci 49:3544–3550. https://doi.org/10.1167/iovs.08-1798

52. Kondo M, Miyake Y, Horiguchi M et al (1998) Recording multifocal electroretinogram on and off responses in humans. Invest Ophthalmol Vis Sci 39:574–580

53. Hood DC, Bach M, Brigell M et al (2012) ISCEV standard for clinical multifocal electroretinography (mfERG) (2011 edition). Doc Ophthalmol 124:1–13. https://doi.org/10.1007/s10633-011-9296-8

54. Hood DC, Seiple W, Holopigian K et al (1997) A comparison of the components of the multifocal and full-field ERGs. Vis Neurosci 14:533–544. https://doi.org/10.1017/s0952523800012190